

## Distinct functional stoichiometry of potassium channel $\beta$ subunits

JIA XU\*<sup>†</sup>, WEIFENG YU\*<sup>†‡</sup>, JERRY M. WRIGHT\*, RONALD W. RAAB<sup>§</sup>, AND MIN LI\*<sup>¶||</sup>

Departments of \*Physiology, and <sup>¶</sup>Neuroscience, The Johns Hopkins University School of Medicine, 725 North Wolfe Street, Baltimore, MD 21205; and <sup>§</sup>Department of Molecular Biology, Affymax Research Institute, Palo Alto, CA 94304

Communicated by Lily Yeh Jan, University of California School of Medicine, San Francisco, CA, December 16, 1997 (received for review November 17, 1997)

**ABSTRACT** Shaker-type potassium channels play important roles in determining the electrical excitability of cells. The native channel complex is thought to be formed by four pore-forming  $\alpha$  subunits that provide four interaction sites for auxiliary modulatory Kv $\beta$  subunits. Because Kv $\beta$  subunits possess diverse modulatory activities including either up-regulation or down-regulation of potassium currents, differential assembly of the  $\alpha$ - $\beta$  complex could give rise to diverse current properties. However, the detailed physical and functional stoichiometry of the  $\alpha$ - $\beta$  complex remains unknown. Kv $\beta$ 1 subunits reduce potassium currents through inactivation, whereas Kv $\beta$ 2 subunits enhance potassium currents by inhibiting the Kv $\beta$ 1-mediated inactivation and at the same time by promoting the surface expression of certain potassium channels. In this report we show that Kv $\beta$ 1 and Kv $\beta$ 2 of the Shaker-type potassium channels display distinct functional stoichiometry to interact with the Kv1  $\alpha$  subunits, a subfamily of Shaker-type potassium channels. The interaction of Kv $\beta$ 1 subunits with  $\alpha$  subunits is consistent with the  $\alpha_4\beta_n$  model, where  $n$  equals 0, 1, 2, 3, or 4, depending upon the relative concentration of  $\alpha$  and  $\beta$  subunits. The  $\alpha_4\beta_n$  stoichiometry allows for gradual changes of the Kv $\beta$ 1-mediated inactivation. In contrast, Kv $\beta$ 2 subunits self-associate to form oligomers and interact with the  $\alpha$  subunits via  $\alpha_4\beta_4$  stoichiometry, which permits effective multivalent associations with  $\alpha$  subunits. Such distinct functional stoichiometry of Kv $\beta$ 1 and Kv $\beta$ 2 provides a molecular mechanism that is well suited to their contrasting activities of up-regulation or down-regulation of potassium currents.

In the nervous system, potassium currents are essential for regulating membrane potentials, cardiac pacemaking, and neurotransmitter release (1–4). Investigation of the mechanisms involved in regulating potassium ion conduction is, therefore, essential for the full understanding of potassium channels in electrical signaling. One key process that leads to reduction or elimination of potassium currents during depolarization is known as inactivation, which includes fast and slow inactivation. In the Shaker-type potassium channels, fast inactivation is primarily mediated by a cytoplasmic inactivation gate that is thought to close the ion conduction pathway by “plugging” into the opened conduction pore (5–7). Because the inactivation gates can be donated by either the pore-forming  $\alpha$  subunits or auxiliary Kv $\beta$  subunits (6, 8), the degree of inactivation is determined by the presence and number of inactivation gate(s) in a given channel complex. Thus, the composition and stoichiometry of  $\alpha$ - $\beta$  complexes could ultimately determine channel inactivation properties.

A total of nine genes encoding various Kv $\beta$  subunits have been reported (J.X. and M.L., unpublished work). On the basis of amino acid sequence, each member of this class of hydro-

philic subunits can be divided into two parts, a conserved core region and a variable N-terminal region. Evidence from binding and electrophysiological studies in heterologous expression systems has shown that Kv $\beta$  subunits interact selectively with  $\alpha$  subunits. Kv $\beta$ 1, for example, inactivates only a subset of Kv1  $\alpha$  subunits through specific interaction with the NAB domain, a conserved region within the N-terminal hydrophilic domain that is also involved in  $\alpha$ - $\alpha$  association (10, 11). The assembly and inactivation of Kv $\beta$ 1 subunits are thought to be mediated by two separable interactions: (i) NAB of  $\alpha$  subunits to the core region of  $\beta$  subunits and (ii) interaction gates of  $\beta$  subunits with their receptors on  $\alpha$  subunits. In contrast, Kv $\beta$ 2, although it also interacts with the Kv1 subfamily of  $\alpha$  subunits, displays no modulatory activity on fast inactivation of  $\alpha$  subunits by itself. Instead, Kv $\beta$ 2 inhibits the Kv $\beta$ 1-mediated inactivation in transfected cells (12), which could result from either the formation of heteromultimers with Kv $\beta$ 1 or effective competition for the binding sites of  $\alpha$  subunits.

The functional stoichiometry of the  $\beta$  subunit of Shaker-type potassium channels in fast inactivation is unknown. The current view of the stoichiometry of the  $\alpha$ - $\beta$  complex is based primarily on two lines of evidence. (i) Hydrodynamic studies show experimentally that the native Kv1.2–Kv $\beta$ 2 complex is consistent with an  $\alpha/\beta$  molar ratio of 1:1 (13), suggestive of  $\alpha_4\beta_4$  stoichiometry because a functional channel formed by  $\alpha$  subunits is a tetramer (14, 15). (ii) Because Shaker-type  $\alpha$  subunits and  $\beta$  subunits are two groups of homologous proteins (8, 16–22), the  $\alpha_4\beta_4$  model is assumed to apply to all  $\alpha$ - $\beta$  complexes in Shaker-type potassium channels.

If the above  $\alpha_4\beta_4$  model were correct, a cell that contained an excess amount of a noninactivating Kv1  $\alpha$  subunit and an inactivating Kv $\beta$ 1 subunit should possess two populations of assembled channels:  $\alpha_4$  and  $\alpha_4\beta_4$ . Electrophysiological analysis should, therefore, show a summation of inactivating current of  $\alpha_4\beta_4$  and noninactivating of  $\alpha_4$ . At the molecular level, the model would predict that the  $\beta$ - $\beta$  interaction is necessary to determine the  $\alpha_4\beta_4$  stoichiometry because  $\alpha$  subunits can form functional channels in the absence of  $\beta$  subunits. In this study, we have directly tested the  $\beta$ - $\beta$  interactions and mapped regions that mediate the interaction by using the yeast two-hybrid system. The functional stoichiometry of  $\alpha$ - $\beta$  complexes was examined by electrophysiological analyses of various wild-type and chimeric  $\beta$  subunits. Our results showed that Kv $\beta$ 1 and Kv $\beta$ 2 interact with  $\alpha$  subunits via two distinct functional stoichiometries:  $\alpha_4\beta_n$  for Kv $\beta$ 1 and  $\alpha_4\beta_4$  for Kv $\beta$ 2. These two modes of subunit interaction may play a role in their contrasting physiological functions *in vivo*.

### MATERIALS AND METHODS

**Methods for the Yeast Two-Hybrid System.** The procedures were performed according to a published protocol (23) by

<sup>†</sup>J.X. and W.Y. contributed equally to this work.

<sup>‡</sup>Present address: ICAgen, Inc., P.O. Box 14487, Research Triangle, NC 27709.

<sup>||</sup>To whom reprint requests should be addressed at: Department of Physiology, The Johns Hopkins University School of Medicine, 725 North Wolfe Street, WBSB 216, Baltimore, MD 21205. e-mail: min.li@qmail.bs.jhu.edu.

The publication costs of this article were defrayed in part by page charge payment. This article must therefore be hereby marked “advertisement” in accordance with 18 U.S.C. §1734 solely to indicate this fact.

© 1998 by The National Academy of Sciences 0027-8424/98/951846-6\$2.00/0 PNAS is available online at <http://www.pnas.org>.

using the HF7c yeast strain (*MAT $\alpha$  ura3-52 his-200 ade2-101 lys2-801 trp1-901 leu2-3,112 gal4-542 gal80-538 LYS2::GAL1<sub>UAS</sub>-GAL1<sub>TATA</sub>-HIS3 URA3::GAL4<sub>17 mer(x3)</sub>-CYCL<sub>TATA</sub>-lacZ*) as host cells; this strain was provided by the laboratory of David Beach (24).

**Vector Construction.** Plasmid constructions were performed according to standard recombinant DNA techniques that we have previously described (12). The expression of cDNAs encoding partial or entire  $\alpha$  subunits in COS cells was driven by the cytomegalovirus promoter using the pCMV vector (Invitrogen) or its derivatives. Kv $\beta$ 1 and deletions of Kv $\beta$ 2 were tagged with the 12CA5 monoclonal epitope as described (11, 12). Construction of the ShB $\Delta$ (6-46) $\Delta$ (59-95) was carried out as follows: First, two *Hind*III sites were introduced into the ShB $\Delta$ (6-46) coding sequence at amino acid positions 59 and 227 as described (25). The coding sequence between amino acids 95 and 227 was amplified by high-fidelity PCR and ligated in the frame between amino acid positions 59 and 227, which resulted in ShB $\Delta$ (6-46) $\Delta$ (59-95). Chimeric Kv $\beta$  subunits were constructed by first cloning the sequence for amino acids 1-72 of Kv $\beta$ 1 into the vector and then inserting either the C-terminal region or the full-length Kv $\beta$ 2 after it. Sequences of oligonucleotides used for constructing the deletion and chimeric constructs are available upon request from the authors. All constructs used in the experiments have been confirmed by DNA sequencing.

**Transient Expression of Potassium Channel Subunits.** COS cells were used for our current studies. Culture of COS cells, plasmid purification, and transfection were carried out as described (11). Cotransfection of Shaker  $\alpha$  subunits and Kv $\beta$ 1, unless otherwise indicated, was done at a ratio of 1:6 (3  $\mu$ g of ShB and 18  $\mu$ g of Kv $\beta$ 1). A plasmid containing CD4 (2  $\mu$ g) marker gene was cotransfected to aid the identification of the transfected cells. Whole-cell recordings were carried out 36-72 h after transfection.

**Whole-Cell Patch-Clamp Recording.** Whole-cell voltage-clamp recordings were carried out according to the published protocol (26). Electrodes (Kimble Glass, Vineland, NJ) were pulled from a two-stage vertical puller (Narishige, Tokyo). When filled with intracellular solution, their resistance varied from 2 to 8 M $\Omega$ . The intracellular solution contained 110 mM KF, 30 mM KCl, 5 mM NaCl, 2 mM MgCl<sub>2</sub>, 10 mM EDTA, and 10 mM HEPES; the pH was adjusted to 7.2 with KOH. During recording, the cells were constantly superfused with the extracellular solution containing 145 mM NaCl, 5.4 mM KCl, 1.8 mM CaCl<sub>2</sub>, 33 mM glucose, and 25 mM HEPES; the pH was adjusted to 7.4 with NaOH. The liquid junction potential was calculated to be 7.13 mV by using JPCALC software (27) and corrected for the holding potential. The current response to a voltage step from a holding potential of -77 mV to 13 mV is illustrated unless otherwise mentioned.

An Axopatch 200A (Axon Instruments, Foster City, CA) amplifier was used in the experiments. Whole-cell capacitance and series resistance were compensated. Voltage protocols were generated by PCLAMP6 software (Axon Instruments). Typically, the cell was held at -77 mV and the holding voltage was then jumped up from this potential to +73 mV in 10-mV increments for 300 ms. Current data were filtered at 1 KHz, digitized at 100- $\mu$ s intervals and stored in a computer (Dell, 486/33) for later analysis. Data analysis was done by using CLAMPFIT (PCLAMP6, Axon Instruments). Basal leak current was subtracted. Data were then transferred into a SIGMA plot (Jandel, San Rafael, CA) for final analysis.

**Mathematical Treatment.** Prediction of the time constant-steady-state current ( $I_{ss}$ )/peak current ( $I_{pk}$ ) curve was done according to the following simplified model previously proposed by MacKinnon and coworkers (15, 28):

$$O \xrightarrow{mk_i} I,$$

where  $m$  is the number of Kv $\beta$ 1 inactivation particles and  $mk_i$  is the inactivation rate constant for channels with  $m$  inactivation particles. We have performed outside-out patch recording and found that inactivation constant did not change in as long as 30 min. The recovery rate, which is in the range of one to several minutes (data not shown), is negligible. Denoting  $A(m)$  as the fraction of channels with  $m$  inactivation particles, then the time constant of any cell is a weighted average of channels with all possible time constants:

$$\tau = \frac{\sum_{m=1}^4 \left[ \frac{A(m)}{mk_i} \right]}{\sum_{m=1}^4 A(m)},$$

where  $\tau_4$  denotes the inactivation time constant for channels with four inactivation gates; we used  $\tau_4 = 12.5$  ms in our calculations, which reflects an averaged inactivation time constant from traces with  $I_{ss}/I_{pk}$  less than 0.4.  $I_{ss}/I_{pk}$  indicates the ratio of steady-state current over peak current, or the proportion of noninactivating current can be given by  $A(0) + f$  ( $f$  is between 0.2 and 0.3 under our recording conditions), where  $f$  is a correction factor for systematic noninactivating current. For a model where each individual inactivation gate acts independently, a simple binomial distribution (see the formula below) was used to assess  $A(m)$ , where  $P$  is the probability of finding one  $\beta$  subunit associating with a given  $\alpha$  subunit.

$$A(m) = C_4^m P^m (1 - P)^{4-m}.$$

For the cooperative  $\alpha$ - $\beta$  association model (i.e.,  $\alpha_4\beta_4$ ) to demonstrate the degree of cooperativity, a binomial distribution was weighted against a linear input of tetramer portion, i.e.,  $A(4)$  was allowed to be changed until the best fit was obtained. Multiple fitting trials have been tested. Four multiple fitting trials are shown in Fig. 4: the  $\alpha_4\beta_4$ (2500) is derived from an  $A(4)$  input with 2,500 times that of the binomial distribution; the  $\alpha_4\beta_4$ (250) is derived from an  $A(4)$  input with 250 times that of the binomial distribution; the  $\alpha_4\beta_2$ (2) is derived from an  $A(2)$  input with half of the oligomers in the  $\alpha_4\beta_2$  stoichiometry. A moderate change of  $A(2)$  caused significant deviation from our experimental data, suggesting that the tetrameric contribution is dominant.

## RESULTS

**Heterogeneity of  $\alpha$ -Kv $\beta$ 1 Stoichiometry.** Kv $\beta$ 1 and Kv $\beta$ 2 appear to show contrasting modulatory activity on potassium currents (see Introduction). To test the  $\beta$ - $\beta$  interaction, we cloned the full-length cDNA of Kv $\beta$ 1 and Kv $\beta$ 2 into a yeast expression vector and tested their interaction in different pairwise combinations by the yeast two-hybrid system (23, 29, 30). In this experiment, Kv $\beta$  subunits were expressed as fusion proteins with either the DNA binding domain or transactivation domain of GAL4. If two Kv $\beta$  subunits could associate, the resultant interaction confers the ability of the yeast transformants to grow on synthetic medium lacking histidine. Fig. 1, columns 1-4, respectively, shows the results of four combinations: Kv $\beta$ 1/Kv $\beta$ 1, Kv $\beta$ 1/Kv $\beta$ 2, Kv $\beta$ 2/Kv $\beta$ 1, and Kv $\beta$ 2/Kv $\beta$ 2. In the absence of  $\alpha$  subunits, Kv $\beta$ 2 could interact either homomerically with Kv $\beta$ 2 or heteromerically with Kv $\beta$ 1. In contrast, no growth was observed for the Kv $\beta$ 1/Kv $\beta$ 1 combination, which is consistent with no interaction (Fig. 1). The failure to observe the Kv $\beta$ 1-Kv $\beta$ 1 interaction raises the question of whether Kv $\beta$ 1 interacts with  $\alpha$  subunits in a stoichi-

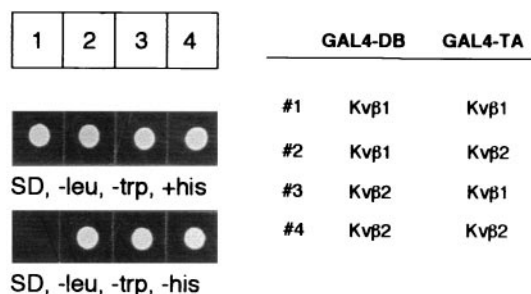


FIG. 1. Differential interactions of Kvb1 and Kvb2. HF7C yeast cells were transformed by pairwise combinations of the yeast two-hybrid constructs that express fusion proteins of either the DNA binding domain of GAL4 (DB) or the transcription activation domain of GAL4 (TA) (Right). Yeast transformants carrying the two fusion proteins were first selected by dextrose synthetic drop-out medium lacking leucine and tryptophan (Left) (SD, -leu, -trp, +his) to confirm that the transformants had taken both plasmids. An identical number of cells from each transformation were inoculated on the same medium lacking histidine (Left) (SD, -leu, -trp, -his). The cells were allowed to grow at 30°C for 48 h.

ometry different from the proposed  $\alpha_4\beta_4$  model of the  $\alpha$ -Kvb2 complex.

There are at least two possible modes by which Kvb1 may interact with the  $\alpha$  subunit. One is through  $\alpha_4\beta_4$  stoichiometry, and the other is through  $\alpha_4\beta_n$  ( $n = 0, 1, 2, 3, 4$ ) stoichiometry. In the first case, when the noninactivating  $\alpha$  subunit is present in excess, one should see a fixed inactivation rate regardless of the  $\alpha_4/\alpha_4\beta_4$  ratio. The variation of the  $\alpha_4/\alpha_4\beta_4$  ratio would only change the level of steady-state current. Under the same conditions, the latter case would give rise to a different inactivation constant depending upon the expression level of Kvb1 in reference to the  $\alpha$  subunits. We cotransfected COS cells with two plasmids encoding either Kvb1 or ShB $\Delta$ (6-46), a mutated Shaker potassium channel lacking the intrinsic inactivation gate (6, 31). Because individual transfected cells may have different ratios of uptaken plasmids, the analyses of inactivation kinetics of randomly selected cells may allow one to distinguish the two modes of interaction. When different transfected cells were recorded by whole-cell voltage clamp, we observed inactivation time constants that varied from 8 ms to more than 36 ms (data not shown). Because the ShB $\Delta$ (6-46) normally does not display fast inactivation, the observed variation of inactivation time constant is in agreement with the

heterogeneous assembly of  $\alpha_4$  with various numbers of  $\beta$  subunits.

The  $\alpha_4\beta_n$  model would predict dosage-dependent inactivation by Kvb1. Thus, within a given cell, higher Kvb1 expression would result in a higher percentage of  $\alpha_4\beta_4$  and  $\alpha_4\beta_3$  and thereby the cell would exhibit faster inactivation. If, however, there were fewer Kvb1 present, the inactivation should be slower because more complexes would be in the forms of  $\alpha_4\beta_1$  and  $\alpha_4\beta_0$ . To test this, we performed experiments by transfecting COS cell with ShB $\Delta$ (6-46) and Kvb1 in two plasmid input ratios, 3  $\mu$ g/18  $\mu$ g (1:6) and 3  $\mu$ g/3  $\mu$ g (1:1), respectively. The transfected cells were first examined by immunoblot analysis using antibodies specific for the Kvb1 polypeptide (11, 12), and the higher expression of Kvb1 in the 1:6 transfection was confirmed (data not shown). We recorded 33 transfected cells for the 1:6 input and 66 cells for the 1:1 Kvb1 input. The recorded traces at +13 mV for each cell were analyzed and fit with two exponential functions to obtain inactivation constants. When ShB $\Delta$ (6-46) and Kvb1 were transfected in a 1:6 ratio, we observed that more than 50% of transfected cells had a fast inactivation time constant of less than 18 ms (Fig. 2A). When ShB $\Delta$ (6-46) and Kvb1 are in a 1:1 ratio, less than 25% of cells showed an inactivation time constant of less than 18 ms (Fig. 2B). As the fraction of the inactivating component became smaller, the rate of inactivation became slower, consistent with the  $\alpha_4\beta_n$  model, which predicts that decreasing the availability of the  $\beta$  subunits gradually reduces the inactivation rate.

To further test the  $\alpha_4\beta_n$  hypothesis, we constructed a Shaker deletion mutant, ShB $\Delta$ (6-46) $\Delta$ (59-95), that is insensitive to the Kvb1-mediated fast inactivation as a result of a reduced ability to interact with Kvb1 (Fig. 2C). This mutant is functional and coassembles with ShB $\Delta$ (6-46). We measured the Kvb1-mediated inactivation rates from cells cotransfected with ShB $\Delta$ (6-46) $\Delta$ (59-95), ShB $\Delta$ (6-46), and Kvb1 with a plasmid input of 2  $\mu$ g, 1  $\mu$ g, and 18  $\mu$ g, respectively. Although the ratio of the total  $\alpha$  subunits and Kvb1 was maintained at 1:6, in contrast to the ShB $\Delta$ (6-46)/Kvb1 transfection in Fig. 2A, a large portion of recordings from the triple transfection showed a slow inactivation rate similar to the results of the 1:1 plasmid input (Fig. 2D,  $n = 49$ ). Thus, these results argue in favor of the  $\alpha_4\beta_n$  model.

**Molecular Determinants in  $\beta$ - $\beta$  Interaction.** The failure to detect Kvb1-Kvb1 interaction suggests that they appear to act independently to bind  $\alpha$  subunits. Because Kvb2 can form homomultimers (ref. 12 and Fig. 1) and the amino acid

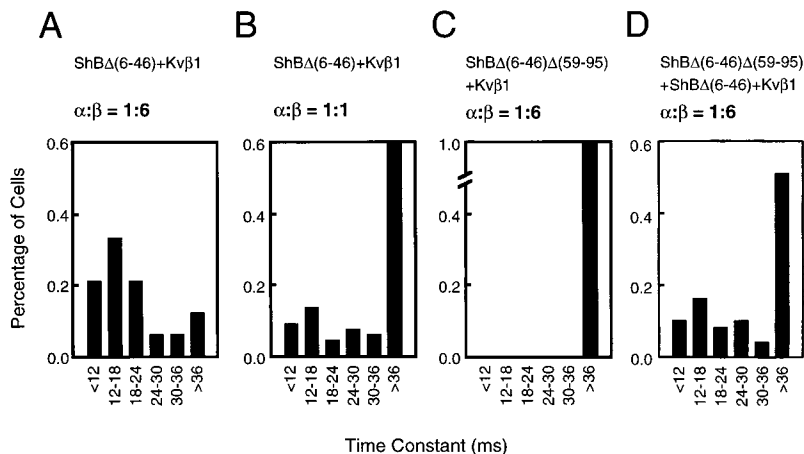


FIG. 2. Distribution of inactivation time constant of the Kvb1-mediated inactivation of ShB $\Delta$ (6-46). The inactivation constants (horizontal axis) were plotted against cell number (in percentage of recorded cells that express Shaker current; vertical axis). The plasmid combinations and  $\alpha/\beta$  ratio of individual transfections are indicated on the top of each histogram. (A) ShB $\Delta$ (6-46) (3  $\mu$ g) + Kvb1 (18  $\mu$ g) ( $n = 33$ ). (B) ShB $\Delta$ (6-46) (3  $\mu$ g) + Kvb1 (3  $\mu$ g) + vector (14  $\mu$ g) ( $n = 66$ ). (C) ShB $\Delta$ (6-46) $\Delta$ (59-95) (3  $\mu$ g) + Kvb1 (18  $\mu$ g) ( $n = 39$ ). (D) ShB $\Delta$ (6-46) (1  $\mu$ g) + ShB $\Delta$ (6-46) $\Delta$ (59-95) (2  $\mu$ g) + Kvb1 (18  $\mu$ g) ( $n = 49$ ).

sequences of Kv $\beta$ 1 and Kv $\beta$ 2 show about 85% amino acid identity at their C-terminal core regions, it would be valuable to know the specific region in Kv $\beta$ 2 that mediates the  $\beta$ - $\beta$  interaction. Previously, we have shown that the C-terminal core region of Kv $\beta$ 2 is the minimal region required for interacting with full-length Kv $\beta$ 2 (12). What is the minimal region of Kv $\beta$ 2 that is sufficient to interact with the core region of Kv $\beta$ 2? To answer this, we constructed a series of deletions of Kv $\beta$ 2 and tested for their ability to interact with either Kv $\beta$ 2 or the core region of Kv $\beta$ 2 [amino acids 39–367, denoted as Kv $\beta$ 2(39–367)] by using the yeast two-hybrid system. The results of growth selection on plates lacking histidine are summarized in Fig. 3. On the basis of these results, we found that the core region of Kv $\beta$ 2 failed to interact with itself. The interaction can be restored when the N-terminal domain is present. One interesting observation is the interaction between Kv $\beta$ 2(1–313) and Kv $\beta$ 2(39–367), which suggests that the N-terminal 313 amino acids of Kv $\beta$ 2 interact with the C-terminal core region. This result implies that the interaction between Kv $\beta$ 2 subunits is not a homophilic interaction since the conserved core regions. Instead, the Kv $\beta$ 2–Kv $\beta$ 2 interaction is polarized and the N-terminal portion of Kv $\beta$ 2 is required to interact with the core region of Kv $\beta$ 2 (Fig. 3). Thus, the failure to form the Kv $\beta$ 1–Kv $\beta$ 1 homomultimer is presumably due to the lack of an appropriate determinant within the N-terminal region that mediates  $\beta$ - $\beta$  interaction in the presence of the conserved core region.

The above binding studies indicate the potential molecular determinants responsible for the difference between Kv $\beta$ 1 and Kv $\beta$ 2 in forming homomultimers. However, one cannot rule out that the two-hybrid interaction results were tainted by the lack of efficient protein folding or sufficient stability for some deletion mutants. To demonstrate this functionally, we constructed two chimeric Kv $\beta$  subunits. One links amino acids 1–71 of Kv $\beta$ 1 (corresponding to the inactivation particle and its putative “chain,” see ref. 8) to the core region of Kv $\beta$ 2 [denoted as  $\beta$ 1(1–72)/ $\beta$ 2(39–367)]; the other fuses Kv $\beta$ 1(1–71) to the full-length Kv $\beta$ 2 [denoted as  $\beta$ 1(1–72)/ $\beta$ 2] (Fig. 4A). Both chimeric constructs contain inactivation particles but differ in their ability to form homomultimers, i.e., only the  $\beta$ 1(1–72)/ $\beta$ 2 chimera can form oligomers and presumably trigger fast inactivation regardless of its expression level with respect to the interacting  $\alpha$  subunits. The Kv $\beta$ 2 express considerably higher than Kv $\beta$ 1 even in an identical vector (12). Transient expression of these chimeric constructs has shown comparable protein level (Fig. 4A). We cotransfected COS cells with ShB $\Delta$ (6–46) plus either of these two constructs in various plasmid inputs to achieve various  $\alpha$ / $\beta$  ratios and performed recordings and analyses similar to those shown in

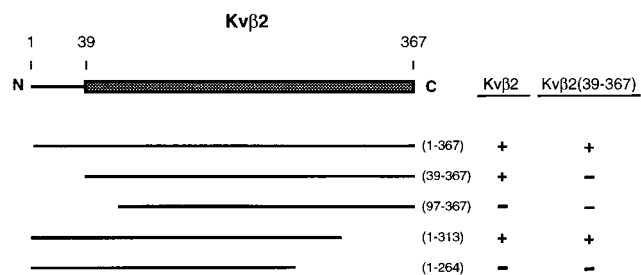


FIG. 3. Molecular determinants that mediate the Kv $\beta$ 2–Kv $\beta$ 2 interaction. (Left) A schematic diagram representing the coding sequence of Kv $\beta$ 2 is shown with the C-terminal core region highlighted as a shaded box. Deletion constructs expressing different coding regions of Kv $\beta$ 2 in GAL4–TA fusions are shown. The numbers in the parentheses indicate the beginning and ending amino acids of the individual deletion mutants. (Right) The ability of the deletion mutants to interact with full-length Kv $\beta$ 2 or Kv $\beta$ 2(39–367) was tested in the yeast two-hybrid system. Results from the growth assay are shown (+, growth; -, no growth).

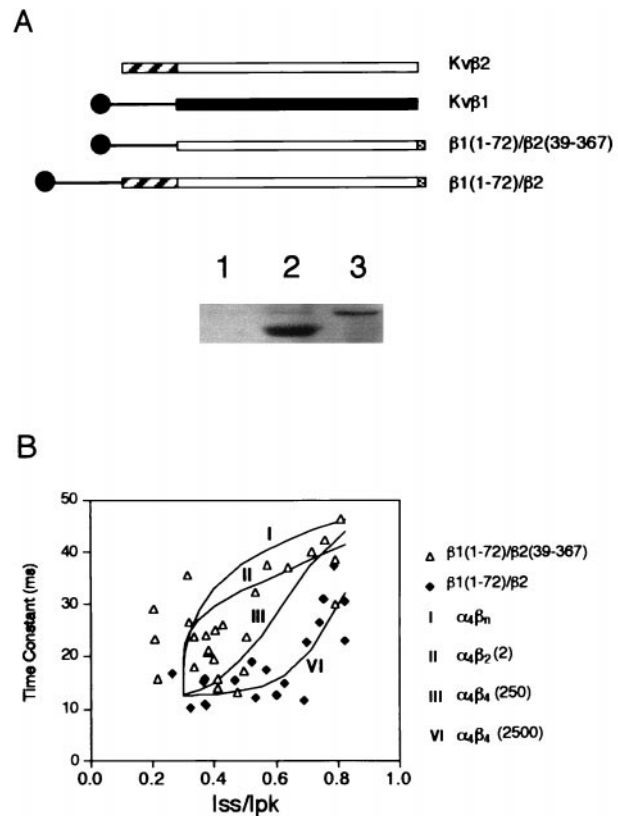


FIG. 4. Inactivation mediated by the chimeric Kv $\beta$  subunits. (A Upper) Schematic diagram showing the coding sequence of Kv $\beta$ 1, Kv $\beta$ 2, and two chimeric constructs. The open or solid boxes represent the core regions of either Kv $\beta$ 2 or Kv $\beta$ 1. The C-terminal shaded boxes show 12CA5 epitope tag. (Lower) Immunoblot showing the monoclonal antibody 12CA5 detection of chimeric  $\beta$  subunit protein from mock-transfected cells (lane 1), cells transfected with  $\beta$ 1(1–72)/ $\beta$ 2(39–367) (lane 2), and cells transfected with  $\beta$ 1(1–72)/ $\beta$ 2 (lane 3). (B) Inactivation time constants in milliseconds obtained from cells transfected with ShB $\Delta$ (6–46) and with chimeric Kv $\beta$  constructs were plotted against  $I_{ss}/I_{pk}$  (steady-state current/peak current).  $\Delta$ , Cotransfection with  $\beta$ 1(1–72)/ $\beta$ 2(39–367) ( $n = 26$ );  $\blacklozenge$ , cells cotransfected with  $\beta$ 1(1–72)/ $\beta$ 2 ( $n = 19$ ). Curves show four fitting trials representing the theoretical prediction of stoichiometry for  $\alpha_4\beta_n$  (I),  $\alpha_4\beta_2$  (2) (II), and  $\alpha_4\beta_4$  under two conditions:  $\alpha_4\beta_4$  is favored by either 250-fold [ $\alpha_4\beta_4$ (250)] (III) or 2,500-fold [ $\alpha_4\beta_4$ (2,500)] (VI) (see Materials and Methods for details).

Fig. 2. The  $\beta$ 1(1–72)/ $\beta$ 2(39–367) chimera inactivates in a mode quite similar to that of the native Kv $\beta$ 1. In contrast, the  $\beta$ 1(1–72)/ $\beta$ 2 chimera showed a significant degree of cooperativity in  $\alpha$ - $\beta$  assembly (Fig. 4). Even at an  $I_{ss}/I_{pk}$  value of 0.7 (where only a very low amount of  $\beta$  was present), the inactivation time constant is still as fast as that obtained at an  $I_{ss}/I_{pk}$  value of 0.2 (see Fig. 4 and Materials and Methods for mathematical fitting). This result and the binding data support the idea that the ability to form a  $\beta$ - $\beta$  multimer allows for cooperative assembly and accelerated inactivation. It also provides evidence that the poorly cooperative  $\alpha_4\beta_4$  assembly of wild-type Kv $\beta$ 1 is due to the lack of Kv $\beta$ 1–Kv $\beta$ 1 interaction.

## DISCUSSION

The composition and stoichiometry of the  $\alpha$ - $\beta$  complex of Shaker-type potassium channels ultimately determine the kinetic and gating properties of the resultant channel protein. In this report, we have presented several lines of evidence supporting the model that Kv $\beta$ 1 and Kv $\beta$ 2, two abundant and homologous  $\beta$  subunits that interact with the same subset of  $\alpha$  subunits, coassemble with  $\alpha$  subunits via two distinct modes.

The Kv $\beta$ 1 subunit binds to  $\alpha$  subunits through a model consistent with  $\alpha_4\beta_n$  stoichiometry, where  $n = 0, 1, 2, 3, 4$ , depending upon the relative concentration of  $\alpha$  and  $\beta$  subunits. In contrast, the Kv $\beta$ 2 subunits form oligomers (probably tetramers) and interact with  $\alpha$  subunits via  $\alpha_4\beta_4$  stoichiometry.

#### Distinct Functional Stoichiometry of Kv $\beta$ 1 and Kv $\beta$ 2.

Three lines of evidence have been presented in support of the notion that Kv $\beta$ 1 does not oligomerize efficiently. As a result, it acts on  $\alpha$  subunits independently depending upon its concentration relative to the expression level of  $\alpha$  subunits. (i) We failed to detect the Kv $\beta$ 1–Kv $\beta$ 1 interaction in the yeast two-hybrid system. Kv $\beta$ 1 interacts with Kv $\beta$ 2 and N-terminal domains of the Kv1  $\alpha$  subunits under the same conditions. It is therefore unlikely that the inability to detect the Kv $\beta$ 1–Kv $\beta$ 1 interaction is due to a technical error such as a failure of GAL4–Kv $\beta$ 1 fusion to enter the nucleus in yeast. (ii) The speed of inactivation correlates with the Kv $\beta$ 1 plasmid input in the cotransfection. This argues against the  $\alpha_4\beta_4$  model, which predicts that inactivation constants should be similar regardless of the expression level of Kv $\beta$ 1. (iii) A channel containing both Kv $\beta$ 1-sensitive and -insensitive  $\alpha$  subunits exhibits much reduced inactivation even under the condition of the high Kv $\beta$ 1 plasmid input.

The inactivation properties of Kv $\beta$ 1 in many ways are similar to that mediated by intrinsic inactivation gates of  $\alpha$  subunits. However, it should be noted that there are several differences between these two types of inactivation gates. For example, the off-rate of the Kv $\beta$ 1 inactivation gate is on the order of seconds (data not shown) in contrast to the 50 ms reported for ShB (28). In addition, a weak Kv $\beta$ 1–Kv $\beta$ 1 interaction was implicated because the rate of recovery from inactivation correlates with the number of Kv $\beta$ 1 inactivation gates (data not shown).

In contrast, the Kv $\beta$ 2 subunits self-associate and presumably form a tetramer. This was first suggested by hydrodynamic studies of the native preparation (13) and later Kv $\beta$ 2 was found to interact in the yeast two-hybrid system in the absence of  $\alpha$  subunits (12). In this report, the formation of Kv $\beta$ 2 oligomers was further demonstrated by two sets of experiments. (i) The determinants that mediate the Kv $\beta$ 2–Kv $\beta$ 2 interaction were tested in the yeast two-hybrid system. Interestingly, the formation of Kv $\beta$ 2 oligomers is not through homophilic interac-

tions. Instead, the Kv $\beta$ 2–Kv $\beta$ 2 association is the result of “polarized” interactions. This result provides a molecular explanation as to why Kv $\beta$ 1 does not interact with itself to form an oligomer. (ii) The Kv $\beta$ 2–Kv $\beta$ 2 interaction was implicated functionally by using a chimeric construct that transplants the inactivation gate of Kv $\beta$ 1 to Kv $\beta$ 2. The resultant chimera has shown strong cooperative  $\alpha_4\beta_4$  assembly regardless of the expression level of  $\beta$  subunits. In fact, our data can be fitted by a model that favors cooperative tetrameric assembly of the  $\beta$  chimera by a factor of 2,500-fold over an independent assembly model (see *Materials and Methods*).

Thus, we propose a working model, which is illustrated in Fig. 5. In a cell that contains both  $\alpha$  subunits and Kv $\beta$ 1 subunits, depending upon the  $\alpha/\beta$  ratio, the channels can be occupied by from zero up to four Kv $\beta$ 1 subunits (Fig. 5A). If all  $\alpha$  subunits, Kv $\beta$ 1 and Kv $\beta$ 2 subunits are present in a given cell or neuron, in principle, we should expect several states (Fig. 5), depending on the  $\alpha/\text{Kv}\beta$ 1/ $\text{Kv}\beta$ 2 ratio. Under this condition, because Kv $\beta$ 2 is capable of forming oligomers, it conceivably has higher avidity to interact with  $\alpha$  subunits as a result of multivalent interactions. If this were the case, the intermediate states (I–IV) would not exist or would be present at a very low level. All  $\alpha$  subunits would be occupied by tetrameric Kv $\beta$ 2 subunits (Fig. 5B, state V). Indeed, coexpression of Kv $\beta$ 1 and Kv $\beta$ 2 in transfected cells showed that Kv $\beta$ 2 completely inhibits the Kv $\beta$ 1-mediated inactivation and that intermediate inactivation cannot be observed (12). It should be noted that the proposed model is simplified. For example, one can speculate that Kv $\beta$ 2 could form linear polymers with more than four subunits. This hypothesis can be tested by a number of ways including biochemical analyses of purified Kv $\beta$ 2 protein. In addition, the difference of Kv $\beta$ 1 and Kv $\beta$ 2 in  $\beta$ – $\beta$  interaction may be further influenced by differential posttranslational modifications, such as phosphorylation, and by other channel-interacting proteins or subunits.

**Molecular Interplay of Kv $\beta$ 1- and Kv $\beta$ 2-Mediated Modulation.** Both Kv $\beta$ 1 and Kv $\beta$ 2 bind to the N-terminal domains of Kv1  $\alpha$  subunits (10–12). So far three Kv $\beta$ 1 splice variants have been identified, known as Kv $\beta$ 1.1, Kv $\beta$ 1.2, and Kv $\beta$ 1.3 (17, 18, 32). These three splice variants have identical C-terminal core regions but differ in the sequence and length of

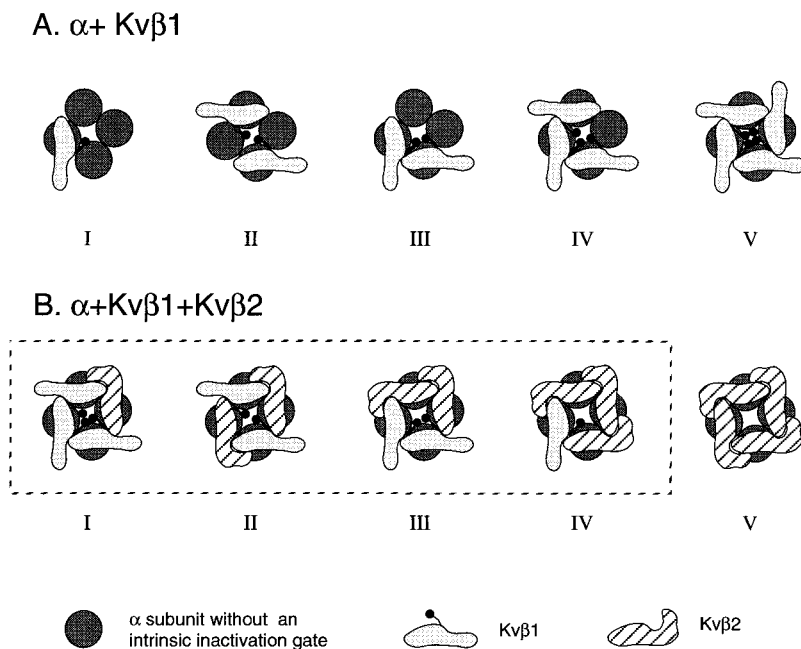


FIG. 5. Proposed stoichiometry of  $\alpha$ – $\beta$  complexes. (A) Diagram illustrating the  $\alpha$ –Kv $\beta$ 1 complexes with increasing availability of Kv $\beta$ 1. (B) Diagram illustrating the possible  $\alpha$ –Kv $\beta$ 1–Kv $\beta$ 2 complexes. The model may not represent the steady-state species of the  $\alpha$ – $\beta$  complexes (see *Discussion*).

their N-terminal domains. Their shared C-terminal core region mediates the interaction with  $\alpha$  subunits and Kv $\beta$ 2, although the distinct N-terminal domains appear to be responsible for conferring the heterogeneity of their modulatory activity. In contrast to Kv $\beta$ 1, the Kv $\beta$ 2 subunit exhibits little modulation on fast inactivation. Instead, it seems to play a role in facilitating surface expression of certain  $\alpha$  subunits (9). More importantly, Kv $\beta$ 2 is capable of inhibiting the Kv $\beta$ 1-mediated inactivation (12).

The heterogeneity of Kv $\beta$ 1 inactivation, presumably as a result of  $\alpha_4\beta_n$  stoichiometry, offers a mechanism to incrementally strengthen the ability of Kv $\beta$ 1 to accelerate fast inactivation as a result of increasing expression of the Kv $\beta$ 1 subunit. Because the off-rate of the Kv $\beta$ 1 inactivation gates is in the range of seconds (data not shown), the inactivation of Kv $\beta$ 1 subunits could provide a prolonged reduction of potassium currents. In contrast to Kv $\beta$ 1, Kv $\beta$ 2 appears to interact with the  $\alpha$  subunits via  $\alpha_4\beta_4$  stoichiometry, which allows for effective competition for the Kv $\beta$ 1 binding sites on  $\alpha$  subunits, thereby inhibiting the Kv $\beta$ 1-mediated inactivation. Combining the high avidity of the  $\alpha_4$ -Kv $\beta$ 2 interaction with its ability to promote surface expression, the outcome of the Kv $\beta$ 2-mediated modulation is to increase potassium currents. Thus, a difference in the functional stoichiometry of these two overlappingly expressed  $\beta$  subunits provides a molecular mechanism to either up-regulate or down-regulate potassium currents.

We thank Dr. Peter Gillespie and members of the Li lab for critical reading of the manuscript and Robyne Butzner for help with the manuscript preparation. This work is supported by grants (to M.L.) from the National Institutes of Health and the Council for Tobacco Research, Inc. M.L. is an American Heart Association-Pfizer Fellow.

1. Connor, J. A. & Stevens, C. F. (1971) *J. Physiol.* **213**, 21–30.
2. Byrne, J. H. (1980) *J. Neurophysiol.* **43**, 651–668.
3. Rogawski, M. A. (1985) *Trends Neurosci.* **8**, 214–219.
4. Hille, B. (1991) *Ionic Channels of Excitable Membrane* (Sinauer, Sunderland, MA), pp. 58–75, 99–116.
5. Armstrong, C. M., Bezanilla, F. & Rojas, E. (1973) *J. Gen. Physiol.* **62**, 375–391.
6. Hoshi, T., Zagotta, W. N. & Aldrich, R. W. (1990) *Science* **250**, 533–538.
7. Jan, L. Y. & Jan, Y. N. (1992) *Annu. Rev. Physiol.* **54**, 537–555.
8. Rettig, J., Heinemann, S. H., Wunder, F., Lorra, C., Parcej, D. N., Dolly, J. O. & Pongs, O. (1994) *Nature (London)* **369**, 289–294.
9. Shi, G., Nakahira, K., Hammond, S., Rhodes, K., Schechter, L. & Trimmer, J. (1996) *Neuron* **16**, 843–852.
10. Sewing, S., Roeper, J. & Pongs, O. (1996) *Neuron* **16**, 455–463.
11. Yu, W. F., Xu, J. & Li, M. (1996) *Neuron* **16**, 441–453.
12. Xu, J. & Li, M. (1997) *J. Biol. Chem.* **272**, 11728–11735.
13. Parcej, D. N., Scott, V. E. & Dolly, J. O. (1992) *Biochemistry* **31**, 11084–11088.
14. Li, M., Unwin, N., Stauffer, K. A., Jan, Y. N. & Jan, L. Y. (1994) *Curr. Biol.* **4**, 110–115.
15. MacKinnon, R. (1991) *Nature (London)* **350**, 232–235.
16. Scott, V. E., Rettig, J., Parcej, D. N., Keen, J. N., Findlay, J. B., Pongs, O. & Dolly, J. O. (1994) *Proc. Natl. Acad. Sci. USA* **91**, 1637–1641.
17. England, S. K., Uebele, V. N., Shear, H., Kodali, J., Bennett, P. B. & Tamkun, M. M. (1995) *Proc. Natl. Acad. Sci. USA* **92**, 6309–6313.
18. England, S. K., Uebele, V. N., Kodali, J., Bennett, P. B. & Tamkun, M. M. (1995) *J. Biol. Chem.* **270**, 28531–28534.
19. Chouinard, S. W., Wilson, G. F., Schlimgen, A. K. & Ganetzky, B. (1995) *Proc. Natl. Acad. Sci. USA* **92**, 6763–6767.
20. Majumder, K., De Biasi, M., Wang, Z. & Wible, B. A. (1995) *FEBS Lett.* **361**, 13–16.
21. Morales, M. J., Castellino, R. C., Crews, A. L., Rasmusson, R. L. & Strauss, H. C. (1995) *J. Biol. Chem.* **270**, 6272–6277.
22. Fink, M., Duprat, F., Lesage, F., Heurteaux, C., Romey, G., Barhanin, J. & Lazdunski, M. (1996) *J. Biol. Chem.* **271**, 26341–26348.
23. Xu, J., Yu, W., Jan, Y. N., Jan, L. Y. & Li, M. (1995) *J. Biol. Chem.* **270**, 24761–24768.
24. Feilolter, H. E., Hannon, G. J., Ruddell, C. J. & Beach, D. (1994) *Nucleic Acids Res.* **22**, 1502–1503.
25. Li, M., Jan, Y. N. & Jan, L. Y. (1992) *Science* **257**, 1225–1230.
26. Hamill, O. P., Marty, A., Nehre, E., Sakmann, B. & Sigworth, F. J. (1981) *Pfluegers Arch.* **391**, 85–100.
27. Barry, P. H. (1994) *J. Neurosci. Methods* **51**, 107–116.
28. MacKinnon, R., Aldrich, R. W. & Lee, A. W. (1993) *Science* **262**, 757–759.
29. Chevray, P. M. & Nathans, D. (1992) *Proc. Natl. Acad. Sci. USA* **89**, 5789–5793.
30. Fields, S. & Song, S.-K. (1989) *Nature (London)* **340**, 245–246.
31. Zagotta, W. N., Hoshi, T. & Aldrich, R. W. (1990) *Science* **250**, 568–571.
32. McCormack, K., McCormack, T., Tanouye, M., Rudy, B. & Stuhmer, W. (1995) *FEBS Lett.* **370**, 32–36.